which is about 12° for this wing at the Reynolds numbers tested. For given flow conditions and sound frequency, the SPL was increased until suddenly partial attachment occurred over the wing. At $\alpha = 20.25°$ about 2/3 attachment occurred initially while at $\alpha = 23.9°$ only the front 1/3 of the wing was initially attached (see Fig. 1). Once partial attachment occurred the SPL could be greatly decreased, sometimes by as much as 10 db, and the wing properties (C_L, C_D, C_M) would not change. Also, increasing the db level to cause greater attachment changed the wing properties only negligibly. For the case illustrated in Table 1, 100 db was required for an initial 2/3 attachment whereas 124 db was required for full attachment. However, the lift and drag coefficients changed only slightly. In this table the power reduction ratio is the ratio of the power saved due to drag reduction divided by the total speaker power. This ratio obviously is very dependent upon the speaker efficiency but gives an indication of the benefits to be gained from the technique.

The minimum SPL required to fully attach the flow for one flow condition as a function of sound frequency is shown in Fig. 2. Although stall suppression is a continuous function of frequency, as seen by Chang,[11] suppression at certain frequencies is much easier than at others. It is believed that these are the frequencies that assist the linear boundary-layer instability whereas large amplitude sound waves can bypass the linear stability mechanism for transition. Similar results were reported by Pfenninger and Reed.[9]

A summary of the best results obtained thus far under various conditions is given in Table 2. ΔU_{rms} is the velocity fluctuation produced by the sound wave if it can be approximated by a plane wave.[3] The relative velocity fluctuation produced by the sound is generally lower than the tunnel turbulence level (5×10^{-3}). Much more intense sound is required to attach the flow at $\alpha = 23.9°$ than at 20.25°. Also, the power reduction ratio is greatly decreased (see Table 3 for typical values) at the higher angle.

At $\alpha = 20.25°$ the tunnel noise was at times sufficient to produce attachment at the higher Reynolds numbers. The tunnel noise was concentrated at 95 Hz and 120 Hz, with levels of 90 and 93 db, respectively, at 90 fps (105 db total SPL). However, it appeared that only 88 db was required to cause stall suppression (see Fig. 1a). As mentioned previously, single frequency sound is much more likely to cause boundary-layer transition than a continuous sound spectra.[1,3]

The SPL's described in this Note are very high in some cases. However, the tests performed at the Air Force Academy[10] indicate that much lower levels are required to cause boundary-layer attachment if internal sound is used. Future tests will include the use of internal sound.

Conclusion

External sound can cause partial reattachment of the flow about a stalled airfoil, greatly increasing the lift and decreasing the pressure drag. The amount of influence of the sound is dependent upon the sound frequency and sound pressure level, and a minimum SPL occurs for some frequencies.

References

[1] Schubauer, G. B. and Skramstad, H. K., "Laminar-Boundary Layer Oscillations and Transition on a Flat Plate," NACA Rept. 909, 1948.

[2] Bergh, H., "A Method for Visualizing Periodic Boundary Layer Phenomena," *Boundary Layer Research*, IUTAM Symposium, edited by H. Görtler, 1958, pp. 173–178.

[3] Boltz, F. W., Kenyon, G. C., and Allen, C. Q., "The Boundary Layer Transition Characteristics of Two Bodies of Revolution, a Flat Plate, and an Unswept Wing in a Low Turbulence Wind Tunnel," TN D-309, April 1960, NASA.

[4] Brown, F. N. M., *See the Wind Blow*, copyright F. N. M. Brown, 1971, pp. 36, 67.

[5] Brown, F. N. M., private communication and movie films, Austin, Texas, March 1972.

[6] Jackson, F. A. and Heckl, M. A., "Effect of Localized Acoustic Excitation on the Stability of a Laminar Boundary Layer," Rept. 62-362, Aeronautical Research Lab., Wright-Patterson Air Force Base, Ohio, June 1962.

[7] Knapp, E. F. and Roache, P. J., "A Combined Visual and Hot-Wire Anemometer Investigation of Boundary-Layer Transition," *AIAA Journal*, Vol. 6, No. 1, Jan. 1968, pp. 29–36.

[8] Spangler, J. G. and Wells, C. S., "Effects of Free Stream Disturbances on Boundary-Layer Transition," *AIAA Journal*, Vol. 6, No. 3, March 1968, pp. 543–545.

[9] Pfenninger, W. and Reed, V. D., "Laminar-Flow Research and Experiments," *Aeronautics and Astronautics*, Vol. 4, No. 7, July 1966, pp. 44–50.

[10] (Anonymous), "Audio Frequency Boundary Layer Control," Cadet Research Paper, Air Force Academy, Colorado Springs, Colo., 1969.

[11] Chang, P. K., Drag Reduction of an Airfoil by Injection of Sound Energy," *Journal Aeronautical Science*, Vol. 28, No. 9, Sept. 1961, pp. 742–743.

Interpretation of Merged Layer Behavior for Wedges

JUDSON R. BARON*
MIT Lincoln Laboratory, Lexington, Mass.

PROCEEDING downstream from a leading edge there are idealized regimes referred to as kinetic, merged, strong and weak interaction, some of which may be of appreciable extent in a hypersonic flow. The over-all extremes are the well known free molecule flow at the leading edge and the boundary layer with an adjacent inviscid shock layer sufficiently far downstream.

The merged layer portion has received particular attention for sharp flat plates[1,2] in hypersonic flow and Shorenstein[3,4] has provided an extension to wedges and cones which shows rather good agreement with experimental data. He used a local similarity analysis to match both flow variables and their normal gradients at the "interface" between the adjacent shock and boundary-layer structures. The approach is essentially an extension of an earlier flat plate study[2] which correctly indicated departures from strong interaction behavior near a leading edge.

Implicit in Shorenstein's wedge analysis[3] is a generalization of the plate behavior such that a strong interaction always follows the merged region. The generalization proves to be somewhat misleading and the present purpose is a clarification of that point for the specific parameter ranges that were considered as well as qualitatively in general. In view of some important numerical inaccuracies, a secondary purpose relates to the need for caution when applying the summary correlations[3] that were suggested.

A tabulation of results was not included in either Refs. 3 or 4. The exact solutions for pressure and heat transfer were shown graphically for a range of wedge (half) angles, $2° \leqq \theta_b \leqq 20°$, and a single Mach number, surface temperature combination ($M_\infty = 20$, $T_b/T_o = 0.06$, T_o being the stream stagnation temperature) over the interval $40 \leqq \bar{\chi}_\infty \leqq 400$. The interaction parameter $\bar{\chi}_\infty \equiv M_\infty{}^3(C/Re)_\infty{}^{1/2}$ is defined here in terms of freestream conditions, the slant length along the surface in the Reynolds number, Re_∞, and the Chapman-Rubesin constant, $C_\infty = (\mu_b T_\infty)/(\mu_\infty T_b)$. In place of tables or additional graphs an empirical correlation was provided in summary of other numerical results. An accuracy of 5% was claimed within the intervals $20 \leqq M_\infty \leqq 25$, $0.06 \leqq T_b/T_o \leqq 0.15$, and $2° \leqq \theta_b \leqq 20°$.

Received July 15, 1974; revision received September 4, 1974. This work was sponsored by the Department of the Air Force.

Index categories: Supersonic and Hypersonic Flow; Boundary Layers and Convective Heat Transfer—Laminar.

* Professor. Associate Fellow AIAA.

Specifically, the correlation expressions were of the form[3]

$$Z_i \cos\theta_b = G(A_i - B_i \log_{10}\beta_w) \tag{1}$$

in which

$$\beta_w = \left(\frac{T_b}{T_o}\right)^{1/2}\left(\frac{\bar{\chi}_\infty{}^2}{GM_\infty{}^4}\right) \tag{2}$$

$$G = 1 + \tfrac{1}{2}\sin 2\theta_b[\cot(\theta_{\text{shock}} - \theta_b) - \tan\theta_b]$$

and the empirical constants A_i, B_i associated with the Z_i parameters for pressure and heat transfer (Stanton number) are given in Table 1.

Table 1 Correlation parameters and constants

Parameter, Z_i	A_i	B_i
Pressure, $p_b/(\rho u^2\bar{\chi})_\infty$	0.022	0.921
Stanton no., $(M^3St/\bar{\chi}^{3/2})_\infty$	0.001	0.037

Figures 1 and 2 show Shorenstein's[3,4] exact solutions for the one merged set ($M_\infty = 20$, $T_b/T_o = 0.06$) that is now available. His predictions for the leading edge free molecule limits and the downstream strong interaction limits are also included. A relatively good experimental comparison is evident, and each merged layer solution appears to fair smoothly into its strong limit. However, it is to be noted that the far downstream (inviscid limit) wedge surface pressures for $\theta_b = 10°$ and 20° are $(p_b/p_\infty) = 22.4$ and 81.9 respectively. In view of the lesser pressures shown in the merged region for large wedge angles, either "negative" interactions $[p_b < (p_b)_{\text{inviscid}}]$ are present or some portions of the solutions are suspect. In either case some of the strong limit asymptotes are inapplicable. The essential point is that an appropriate measure of interaction strength is the change from a relevant non-interaction level, which here is $(p_b)_{\text{inviscid}}$.

A reinterpretation of the results is possible. In doing so it would be helpful to make use of the full range of solutions implied by Eq. (1). Unfortunately, it proves necessary to append a factor (5.0×10^{-5}) to the right hand side of Eq. (1) to obtain a reasonable "corrected" correlation relation. The resulting correlation prediction is also shown in Fig. 1. Similarly, the Stanton numbers implied by Eq. (1) result in a need for typical correction factors of $0.63(\theta_b = 2°)$ and $0.36(\theta_b = 10°)$ to achieve agreement with the exact solutions in Fig. 2. Lastly, a constraint on the correlation equation was that $\beta_w < 1.0$. In applying Eq. (1) this corresponds to a boundary which falls in the range $2.0 \gtrsim \bar{\chi}_\infty/M_\infty{}^2 \gtrsim 5.0$ but predicts pressures well below the free molecule levels. A recent *plate* study[6] based on finite difference solutions of the Navier-Stokes equations extends merging as far upstream as $\bar{\chi}_\infty/M_\infty{}^2 \cong 15$ to essentially the free molecule asymptotic value. For $M_\infty = 10.0$ the decay (proceeding upstream from the peak at $\bar{\chi}_\infty/M_\infty{}^2 \cong 1$) in pressure occurs quite gradually in contrast to the abrupt changes suggested by Eq. (1). For these several reasons the remaining remarks are restricted solely to the *exact* solutions for $M_\infty = 20$ depicted in Figs. 1 and 2. The accuracy of Eq. (1) for other conditions with or without the mentioned corrections is unclear.

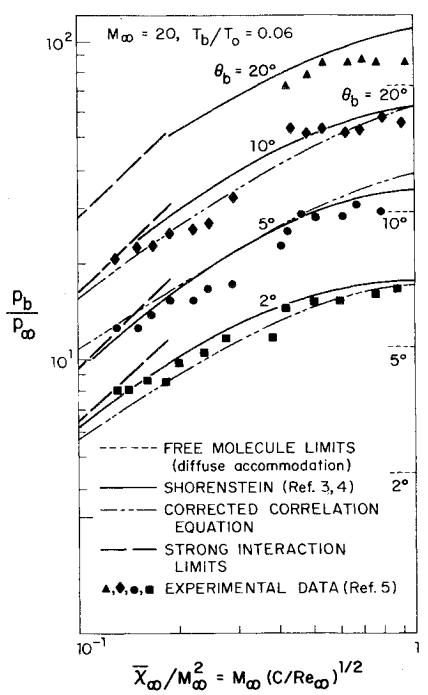

Fig. 1 Surface pressure for wedges.

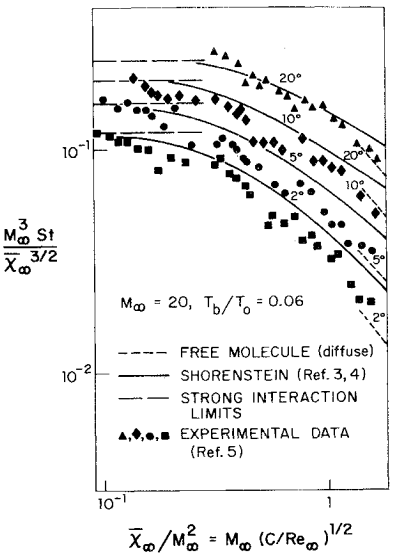

Fig. 2 Heat transfer rate for wedges.

Despite the correlation discrepancies, the exact solutions in Figs. 1 and 2 do furnish the necessary merged layer behavior to permit a re-evaluation. The viewpoint adapted in Figs. 3 and 4 is that of departures from noninteracting-pressure and weak-interaction-heat-transfer levels far from the leading edge. The relevant interaction parameter, $\bar{\chi}_w$, is that associated with the downstream wedge conditions, or what may be considered to be an *equivalent plate* interaction parameter. The objective is to isolate any departure from interaction theory that arises specifically from the merging process as a result of the development of shocks of varying strengths.

Thus

$$\frac{\bar{\chi}_w}{\bar{\chi}_\infty} = \left(\frac{M_w}{M_\infty}\right)^3\left(\frac{(C/Re)_w}{(C/Re)_\infty}\right)^{1/2} \tag{3}$$

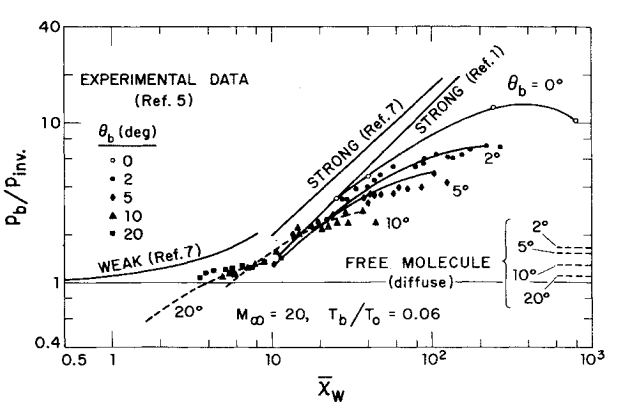

Fig. 3 Wedge surface pressure on equivalent flat plate basis.

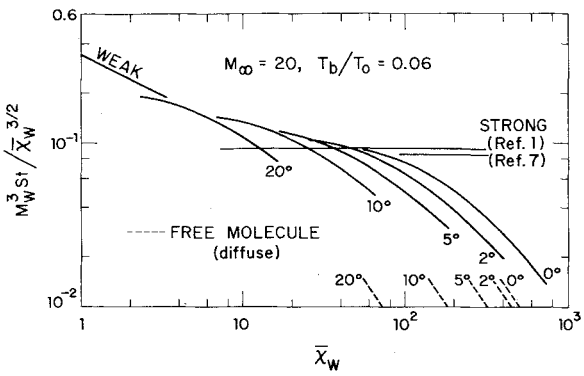

Fig. 4 Wedge heat transfer rate on equivalent flat plate basis.

and

$$\frac{(M^3St/\bar{\chi}^{3/2})_w}{(M^3St/\bar{\chi}^{3/2})_\infty} = \left[\frac{M_w}{M_\infty}\left(\frac{\bar{\chi}_\infty}{\bar{\chi}_w}\right)^{1/2}\right]^3 \frac{(\rho u)_w}{(\rho u)_\infty} \tag{4}$$

in which $(\ )_w$ implies the use of inviscid conditions downstream of an oblique shock of turning angle θ_b, and $St_\infty = -\dot{q}_b/(\rho u)_\infty(h_o - h_b)$ is the non-dimensional heat transfer flux. Application of Eqs. (3) and (4) to the exact solutions and experimental data of Figs. 1 and 2, and introducing $(p_b)_{\text{inviscid}}$ as the pressure datum, yields the equivalent plate results for each wedge angle (Figs. 3 and 4; $\theta_b = 10°$ and 20° loci are dashed for clearness in Fig. 3). The experimental data in Fig. 3 were plotted from the original source,[5] which indicated a smooth decay to the inviscid wedge limit. The plate ($\theta_b = 0°$) solution is from Ref. 2.

In this form, the merged solutions are seen to be initiated at appreciably decreasing $\bar{\chi}_w$ as shock strength (i.e., θ_b) increases. The peak pressure interaction proves to be much weaker for thicker wedges. The experimental points confirm the theoretical trends (as expected in view of Figs. 1 and 2) but clearly extend into the weak interaction region and provide no evidence of a "negative" interaction. The portion of the $\theta_b = 20°$ curve for $(p_b)/(p_b)_{\text{inviscid}} < 1$ and the implied extrapolation of at least the 10° curves suggest a failure of Shorenstein's method[3] at sufficiently small $\bar{\chi}_w$. Nevertheless, the larger θ_b solutions do properly approximate the data band in the transition between the strong and weak regimes. The experimental points have been omitted from Fig. 4 for clarity but again are comparably clustered along the exact solutions as in Fig. 2.

In general, smaller interaction effects were to be expected for wedges in contrast to a plate as a result of the strong inviscid pressure field.[7] Effectively, the lesser $\bar{\chi}_w$ (e.g., $\bar{\chi}_w/\bar{\chi}_\infty \cong 0.1$ for $\theta_b = 10°$) contracts the (dimensional) distance within which the interaction is important. In addition, however, Figs. 3 and 4 illustrate the weakening that results from the merging process for stronger shocks. It is clear that for large wedge angles ($\theta_b \approx 20°$) the strong regime is virtually eliminated.

References

[1] Pan, Y. S. and Probstein, R. F., "Rarefied Flow Transition at a Leading Edge," *Fundamental Phenomena in Hypersonic Flow*, Cornell University Press, Ithaca, N.Y., 1966, pp. 259–306.

[2] Shorenstein, M. L. and Probstein, R. F., "The Hypersonic Leading Edge Problem," *AIAA Journal*, Vol. 6, No. 10, Oct. 1968, pp. 1898–1906.

[3] Shorenstein, M. L., "Hypersonic Leading Edge Problem: Wedges and Cones," *AIAA Journal*, Vol. 10, No. 9, Sept. 1972, pp. 1173–1179.

[4] Shorenstein, M. L., "A Hypersonic Merged Layer Model for Sharp Wedges and Cones," Ph.D. thesis, Dept. of Aeronautics and Astronautics, MIT, Cambridge, Mass., Jan. 1971.

[5] Vidal, R. J. and Bartz, J. A., "Surface Measurements on Sharp Flat Plates and Wedges in Low-Density Hypersonic Flow," *AIAA Journal*, Vol. 7, No. 6, June 1969, pp. 1099–1109.

[6] Tannehill, J. C., Mohling, R. A. and Rakich, J. V., "Numerical Computation of Hypersonic Viscous Flow over a Sharp Leading Edge," *AIAA Journal*, Vol. 12, No. 2, Feb. 1974 pp. 129–130.

[7] Hayes, W. D. and Probstein, R. F., *Hypersonic Flow Theory*, Academic Press, New York, 1959.

Model for the Solution of Supersonic Viscous Interaction Effects on Blunted Cones

GABRIEL MILLER* AND ANDREW SROKOWSKI†
New York University, New York, N.Y.

Introduction

THE problem area of low density, supersonic and hypersonic flows over blunted cones has received much theoretical[1–5] and experimental,[6–12] attention over the past decade. The practical application of such investigations: space vehicle re-entry and high altitude flight, has initiated the development of numerous analytical and numerical models to accurately predict the viscous inviscid interaction and its effect on fluid properties, particularly pressure distribution.

A proper assessment of the effects of interaction on blunted surfaces can only be accomplished by a theory which allows for both pressure and vorticity interaction phenomena for the high Mach number, low Reynolds number flows of practical interest. Previous investigations by the authors[13,14] have attempted to establish a model which allows for the inclusion of all interaction effects directly, i.e., by solving the entire viscous and inviscid flowfield at the same time and establishing unique solutions. The model's main features are: its inclusion of viscous transports in the characteristic equations, the matching of the subsonic viscous flow (solved by a second-order, implicit Crank-Nicholson scheme) to the supersonic flow in the transonic zone, the inclusion of the normal momentum equation (thus allowing for transverse pressure gradients, whose importance is increased in thick, high curvature boundary layers), and the solution of the entire interaction problem by a marching technique. It is shown herein that the model's predictions of pressure distribution and heat transfer for high Mach number, low Reynolds number, flows over blunted cones are in excellent agreement with experimental data, whereas other interaction models do not exhibit such accuracy.

Method of Analysis

The calculation of the flowfield is divided into three parts; 1) the subsonic boundary layer, 2) the supersonic region (including viscous transports), and 3) the matching region.

1) Subsonic boundary layer

The equations for the inner, highly viscous, region are represented by the boundary-layer equations in coordinates measured along and normal to the body. Consistent with the hypothesis of moderate Reynolds number, terms of order $[1/(Re_\infty)^{1/2}]$ are retained after coordinate stretching. As normal pressure gradients are impressed on the inner region from the outer (supersonic) flow, and since body curvature may be significant, the normal momentum equation is retained. Thus, for axisymmetric flowfields, the equations are[13,14]

$$(R\rho u)_{\bar{x}} + (\beta R\rho\bar{v})_{\bar{y}} = 0$$

$$\rho[uu_{\bar{x}} + \beta\bar{v}u_{\bar{y}} + \kappa u\bar{v}/(Re_\infty)^{1/2}] + p_{\bar{x}} = S_1'$$

$$\rho[u\bar{v}_{\bar{x}}/(Re_\infty)^{1/2} + \beta\bar{v}\bar{v}_{\bar{y}}/(Re_\infty)^{1/2} - \kappa u^2] + \beta p_{\bar{y}}(Re_\infty)^{1/2} = 0$$

$$\rho(uT_{\bar{x}} + \beta\bar{v}T_{\bar{y}}) - E_\infty(up_{\bar{x}} + \beta\bar{v}p_{\bar{y}}) = S_2'$$

Received July 25, 1974. This work was supported by the Department of the Navy, Office of Naval Research, under Contract N00014-67-A-0467-0021.

Index category: Subsonic and Transonic Flow.

* Associate Professor of Applied Science, New York University.

† Associate Research Scientist, Aerospace Laboratory; presently Engineering Technologist, NASA Langley Research Center, Hampton, Va.